Development of rapid tests for the detection of L-malic acid in wine using enzymes immobilized on paper via carbohydrate-binding modules

Ana Catarina dos Reis Faria[1]

[1]Master Student in Biotechnology at Instituto Superior Técnico, Universidade de Lisboa, Av. Rovisco Pais, 1, 1049-001 Lisboa, Portugal

Abstract Current analysis to detect L-malic acid are complex and time consuming to be performed by winemakers. Microfluidic paper-based devices (µPADs) are characterized by their simplicity and elimination of external equipment. The objective of this work was to develop a colorimetric wax-printed µPAD to detect L-malic acid in wine that is suitable for the winemaking industry. The detection of L-malic acid was based on enzymatic reactions involving L-malate dehydrogenase (MDH) and aspartate aminotransferase (AST) and a non-enzymatic reaction, that result in the formation of a purple compound. The analytical performance of the µPAD using enzymes physically adsorbed or immobilized via affinity interactions onto paper was assessed. Attempts were made to fuse both MDH and AST with the carbohydrate binding module from C. *thermocellum* (CBM3) that has a high affinity towards cellulose. The AST-CBM3 fusion protein was cloned successfully, yielding a fusion with an affinity to cellulose 2-fold higher than AST. Under optimized conditions, the assay is linear between 5-150 mg/L of L-malic acid, with a limit of detection of 5.8 mg/L and 9.2 mg/L, for the assay with AST and AST-CBM3, respectively. Results obtained in the analysis of a range of wines with the device with AST-CBM3 were comparable to the ones obtained with a commercial kit.

Keywords: Microfluidic paper-based analytical device, Colorimetric detection, L-malic acid, Carbohydrate- binding module (CBM), Fusion proteins, Wine

1 Introduction

During winemaking it is essential to monitor the concentration of organic acids, in order to ensure the quality of the final product [1]. L-tartaric and L-malic acids are the main organic acids present in wines, representing 70-90% of its total acidity [2]. Wine acidity affects two of the key drivers for consumers, flavor and aroma. The concentration and nature of organic acids also influences wine's biological stability and ultimately shelf-life. L-malic acid is a complex organic acid that is originated directly from grapes during their development. The balance between L-malic acid synthesis and catabolism in grapes is highly affected by temperature. Grapes in warmer climates have faster rates of L-malic acid degradation than in cold climate regions, so L-malic acid content is usually lower. The content of L-malic acid can range between 1 to 10 g/L depending on grape variety and climate region [2].

In cool-climate regions, the production of high quality wines depends on the optimal adjustment of wine acidity. After alcoholic fermentation, wines must undergo Malolatic Fermentation (MLF) [3] where L-malic acid is de-carboxylated into the weaker L-lactic acid, by malolatic enzymes characteristic of lactic acid bacteria (LAB). This induces wine's deacidification by increasing pH and confers a smoother and fruity flavor [4].

Analytical methods currently used to detect and quantify L-malic acid include spectrophotometry, capillary electrophoresis and chromatography (e.g. high performance liquid chromatography, HPLC) [5] [6] [7]. Although very accurate and precise, these methods rely on sample pre-treatment, are quite

complex, require skilled personal and make use of expensive apparatuses.

Microfluidic paper-based analytical devices (µPADs) were introduced in 2007 by Whiteside's group [8]. µPADs hold significant potential to be applied in winemaking industry due to their simplicity, low cost, low sample volume requirement and portability. Fluid movement in these devices is controlled by capillary-forces, eliminating the need for external pumps. µPADs are fabricated by patterning hydrophobic channel walls, which guide the flow of aqueous solutions. Wax-printing [9] is the simplest, faster and most affordable patterning method. After wax deposition using a common printer, the wax is re-melted with a hot plate, spreading vertically and laterally into the paper. µPADs are suitable for diagnostic applications, environmental monitoring and food quality testing.

Furthermore, µPADs are compatible with colorimetric detection methods and can be functionalized with biomolecules to be specific for a given analyte of interest. Bioaffinity immobilization strategies have been explored by coupling biomolecules with carbohydrate binding-module (CBM) that adhere spontaneously to cellulose [10]. CBMs are non-catalytic domains present in glycoside hydrolases, which target the associated catalytic modules to their substrates, resulting in higher enzyme activity. Based on primary structure similarity, CBMs have been grouped into 71 families (see Carbohydrate Active Enzymes database at http://www.cazy. org). CBM3 from the cellulosomal-scaffolding protein A (CipA) of *Clostridium thermocellum* is responsible for structural organization of the cellulosomes [11]. In addition it has an affinity constant towards cellulose of the order of 10^6 M^{-1} [12]. Previously in our lab, CBM3 was fused with a ZZ domain from protein A and combined with a µPAD for the molecular diagnostics of infectious diseases. This strategy increased substantially the efficiency of the µPAD, since it resulted in a higher intensity and spatial confinement of signals [13].

In this work, a colorimetric µPAD for the detection of L-malic acid in wines suitable for winemaking industry was developed. As a first approach, L-malate dehydrogenase and aspartate aminotransferase were physically adsorbed onto paper together with chromogenic reagents. A wax printing method was implemented and µPAD analytical performance was assessed. To improve µPAD performance and shelf-life, a bioaffinity immobilization strategy was devised to fuse L-malate dehydrogenase and aspartate aminotransferase with CBM3 from *C. thermocellum*.

2 Materials and Methods

Reagents and Materials L-malic acid, D-(+)-trehalose dehydrate, phenazine methosulphate (PMS), 3-(4,5-dimethylthiazol-2-yl)-2,5-diphenyltetrazolium bromide (MTT), imidazole, NaHepes, NaCl, polyvinyl alcohol 98 - 99% hydrolyzed and L-glutamic acid monosodium salt monohydrate were all purchased from Sigma-Aldrich (St. Louis, MO). Tris was from Eurobio (Madrid, Spain) and activated carbon from Merck (Darmstadt, Germany). MDH, ASP and NAD^+ were kindly provided by NZYTech (Lisbon, Portugal). Whatman No.1 chromatography paper was used as the base material for all µPADs. 1% (v/v) polyvinyl alcohol was prepared in pre-heated water at 80 ºC and dissolved for 8 hours and supplemented with 4 drops of Triton X-100 (Merck, Darmstadt, Germany). Standard solutions of L-malic acid were prepared in Millipore-purified water. The following white and red wines were purchased in a local market: 1. Porta da Ravessa white wine; 2. Vinho Regional Alentejano – Pingo Doce white wine, 3. Lezíria white wine, 4. Porta da Ravessa red wine; 5. Vinho Regional Alentejano – Pingo Doce red wine, 6. Lezíria red wine.

Fabrication of µPAD Hydrophobic barriers in the µPADs used in this work where made by wax-printing. Device designs were developed with a drawing software, Inkscape® and printed with a Xerox ColorQube 8570 wax printer using default settings for image-quality printing. After printing, the wax was re-melted on a hot plate at 150

ºC for 2 minutes. In this work, arrays of 6 mm diameter circles with 0.4 mm line thickness and a lateral flow device with 38.7 mm x 6 mm and three compartments, each with 6 mm-diameter and 0.4 mm line thickness, were tested. On the reverse side of the paper, adhesive tape was used as a support to enhance control over fluid flow and prevent leakage during the assay.

Detection of L-malic acid in µPADs µPADs with 6 mm circles were prepared by spotting reagents in the following order: i) 1 µL of 10% trehalose in water; ii) 0.7 µL of 1% polyvinyl alcohol and triton X-100 (4 drops) in water (25 mL); iii) 5 µL of a reagent solution containing 2 %(v/v) aspartate aminotransferase (2 mg/mL with 536 U/mL), 2 %(v/v) L-malate dehydrogenase (2 mg/mL with 3960 U/mL), 9.5 %(v/v) PMS (100 µM), 24 %(v/v) MTT (7.4 mM), 4.8 %(v/v) Tris (1 M) plus L- glutamate (1 M) and 57 %(v/v) Millipore-purified water. This last mixture is hereafter referred to as "mix". After addition of the reagents, spots were allowed to air dry at room temperature for 1 hour. Then, 7 µL of a sample solution containing 51% (v/v) of a L-malic acid standard solution, 20.4% (v/v) Tris plus L-glutamate (1 M) and 28.6% (v/v) NAD^+ (95.5 mM) were added to each spot. Negative controls were used in all assays, where L-malic acid was replaced by Millipore-purified water. After sample uptake, all spots were allowed to dry for 40 minutes and scanned (HP scanjet 4400c scanner) under optimized brightness and contrast settings. All spots were analyzed using ImageJ® software by converting the original image to 8-bit grey scale and inverting black/white pixels. Then, the reaction zone was selected and the mean grey intensity was measured. The size of the circles used to select the reaction zone was kept constant during this work. Moreover, the average mean grey intensity was calculated by discounting the mean grey intensity of the negative control.

Time course stability µPADs were prepared with trehalose, polyvinyl alcohol and triton X-100 and 5 µL of a reagent solution containing all the reagents required for the assay, as described previously. Subsequently, the devices were stored at 4º C and room temperature (RT). During storage, devices were protected from direct light exposure, because both MTT and PMS are light sensitive compounds. Each spot was tested over a period of several days with 7 µL of a solution containing the analyte (0 or 150 mg/L of L-malic acid), Tris plus glutamate and NAD^+.

Detection of L-malic acid using a lateral-flow µPAD The L-malic acid detection method described above was adapted to a lateral flow assay. A lateral flow device with 38.7 mm x 6 mm was used. The µPAD was prepared by adding 1 µL of 10% trehalose in water and 0.7 µL of 1% polyvinyl alcohol and triton X-100 (4 drops) in water (25 mL) to the NAD^+ and reagent zones. Then, 1.5 µL of mix was added to the reaction zone, while 2 x 1 µL of NAD^+ was added to the middle compartment. For sample testing, 28 µL of a sample solution containing 71 %(v/v) of an L-malic acid standard solution and 29 %(v/v) Tris plus L-glutamate (1M) were added to the sample input zone. After air-drying for 40 minutes, the channels were scanned.

Construction of pET21a_AST-CBM3 and pET21a_MDH-CBM3 pET21a_AST, pET21a_MDH plasmids were kindly provided by NZYTech, Lda. pET21a_ZZ-CBM3, previously used in our lab, was genetically modified to introduce one upstream restriction site for XhoI restriction and to remove the stop codon. The gene *cbm3* and its N-terminal linker region were amplified from pET21a_ZZ-CBM3 by PCR using the KOD (Novagen) suggested protocol. The forward primer used was 5'-ggggtaaagaaccgctcgagcaccacca-3' while the reverse primer was 5'-tggtggtgctcgagcggttctttacccc-3'. PCR cycling conditions were performed as follows: preheating at 95 °C for 2 min, 40 cycles at 95 °C for 20 s, 67.1 ºC for 10 s and 70 ºC for 2.4 min. PCR product was digested for 2 hours at 37 ºC using the restriction enzyme XhoI (Thermo scientific), followed by a 1% agarose gel to purify *cbm3* from pET21a_ZZ-CBM3 using a purification kit (NZYTech) according to the manufacturer instructions. pET21a_AST and pET21a_MDH were digested with XhoI, recovered from a 1% agarose gel electrophoresis with a purification kit (NZYTech) and used as vectors in the cloning process. Then, 30 µL of digested plasmid DNA were mixed with 1 µL of alkaline phosphatase (Roche, Basel, Switzerland), 5 µL of buffer and 14 µL of water. Ligation between the vector (pET21a_AST or pET21a_MDH) and the fragment (*cbm3* gene) was performed using a 3:1 insert/vector ratio using T4 ligase (Promega) for 3 hours at room temperature and overnight at 4 ºC. Subsequently, *E. coli* DH5α cells (Invitrogen, Carlsbad, CA) were transformed by

electroporation (2500 V) with 1 µL of ligation mixtures. After purification, the recombinant plasmids were confirmed by XhoI digestion and sequence.

Expression and purification of AST and AST-CBM3 Plasmids pET21a_AST and pET21a_AST-CBM3 were transformed into *E. coli* BL21(DE3) (Novagen), a strain suitable for protein expression. Then, LB media supplemented with 100 µg/mL ampicillin was inoculated with these cells and incubated overnight at 37 ºC, 250 rpm. Subsequently, cells were diluted down to an OD_{600} of 0.1 and inoculated into 500 mL of LB media supplemented with 100 µg/mL ampicillin. This media was incubated at 37 ºC, 250 rpm. At an OD_{600} between 0.4 and 0.6, cells were induced with 1 M of isopropyl β- D-1-thiogalactopyranoside (IPTG) and incubated for 16 hours at 37 ºC (250 rpm). Cells were harvested by centrifugation (Eppendorf centrifuge 5810R) at 4 000 rpm, 4 ºC, for 10 minutes and the pellet was resuspended in 30 mL of loading buffer (10 mM imidazole, 50 mM NaHepes, 1 M NaCl, 5 mM $CaCl_2$, pH 7.5). Cells were then disrupted by sonication (Branson Sonifier 250) for 6 x 30 seconds on ice with interruptions of 30 seconds. Following centrifugation at 15 000 g, 4 ºC, for 15 minutes, the resulting supernatant was filtered using a 0.22 µm syringe filter (Milipore, Milex®- GV).

AST-CBM3 and AST were purified by immobilized metal ion affinity chromatography (IMAC), using a Ni Sepharose™ 6 fast flow (GE Healthcare) column and a peristaltic pump with a flow rate of 1 mL/min (Qlabo). The recovered protein was kept on the elution buffer that contains mainly 300 mM of imidazole and stored at 4 ºC. Purity and molecular weight were confirmed by SDS-PAGE and the concentration was determined by the BCA Protein Assay (Pierce).

Binding of AST-CBM3 to cellulose Two circles of Whatman No.1 chromatography paper with 0.009 g each were introduced into the wells of filter plates (Milipore, MultiScreen-HV 96-well plates with a hydrophilic membrane Durapore 0.45 microns). Then, 100 µL of a solution containing 5 % (v/v) Tris (1 M) plus glutamate (1 M) pH 10 and 95 % (v/v) of Millipore-purified water were added and plates were incubated for 30 min at RT with a shaking rate of 300 rpm to equilibrate the paper. After filtration, 3 µM of AST- CBM3 fusion protein diluted in the previous buffer was added to each well and incubated for 30 min (at RT, 300 rpm). The liquid was then filtered and the concentration of protein before and after filtration was measured using the Pierce® BCA Protein Assay kit. The same protocol was performed for AST and CBM3 controls.

Analytical performance of a µPAD with AST-CBM3 Analytical performance of a µPAD with AST-CBM3 was studied by preparing devices as described previously. Briefly, a solution containing 10 % of trehalose was first added to each spot, followed by a solution containing 1% polyvinyl alcohol and triton X-100. Then, 5 µL of a reagent solution containing 2 %(v/v) AST-CBM3 (2.69 mg/mL), 2 %(v/v) L-MDH, 9.5 %(v/v) PMS (100 µM), 24 %(v/v) MTT (7.4 mM), 4.8 %(v/v) Tris (1 M) plus L- glutamate (1 M) and 57 %(v/v) Millipore-purified water were added. The activity of the AST produced in the lab (in 300 mM of imidazole buffer) was also studied using a similar protocol, but with 11 % (v/v) of AST in the reagent solution to match the molar amounts of enzyme. After addition of the reagents, the spots were allowed to air dry at RT for 1 hour. Next, 7 µL of a sample solution containing 51 %(v/v) L-malic acid solution (with concentrations of 0, 5, 10, 20, 50, 100, 150, 200, 300, 600 mg/L), 20.4 %(v/v) Tris plus L-glutamate (1 M) and 28.6 %(v/v) NAD^+ (95.5 mM) were added to each spot. After 40 minutes of drying at room temperature, the results were recorded using a scanner (HP scanjet 4400c) and a camera (Olympus E-PM1 camera). Mean grey intensity of each spot was measured using ImageJ®. In addition, shelf stability and lateral flow tests were performed as described previously.

L-malic acid detection in wines using a µPAD As a proof of concept, white and red wines were tested using the colorimetric µPAD developed with AST-CBM3. Firstly, red wines were pre-treated with activated carbon, in order to remove its color. Thus, 0.025 g of activated carbon were added to 500 µL of red wine, centrifuged for 3 minutes at 14 000 rpm and filtered using a 0.22 µm seringe filter (Milipore, Milex®- GV). Then, wines without dilution and diluted 5, 10 and 50 times were analyzed for L-malic acid using a µPAD with 6-mm spots. The spots and the samples were prepared as described previously and after 40 minutes of air-drying the µPADs were scanned and the mean grey intensity was measured using ImageJ®.

L-malic acid detection in wines using an UV method To validade the data obtained with the µPAD developed, wine samples were also analyzed using an L-malic acid, UV

detection kit (kindly provided by NZYTech) according with the manufacturer instructions. Wines were diluted 5 and 10 times and the absorbance was measured at 340 nm using a microplate reader (SPECTRAmax PLUS 384) at RT. Standard solutions of L-malic acid prepared in water with concentrations between 5 and 300 mg/L were used on the day of preparation to obtain the calibration curve.

Spiking of samples and analysis using a µPAD Wines number 3 (previously diluted 50 times) and 4 (pre-treated with activated carbon) were spiked with 1.3, 2.5 and 5.0 mg of L-malic acid. Finally, 7 µL of a solution containing 51 %(v/v) of wine spiked, 20.4 %(v/v) Tris plus L-glutamate (1 M) and 28.6 %(v/v) NAD^+ (95.5 mM) were added to spots prepared as described previously. After air-drying and scanning, each spot was analyzed by measuring the mean grey intensity using ImageJ®.

3 Results and Discussion

3.1 Colorimetric bioassay

One of the goals of this work was to develop a colorimetric detection method for L-malic acid and to adapt it to a µPAD. Enzymatic detection was employed, owing to their rapid, selective and hence the great accuracy obtained in the measurements. In the colorimetric system developed (see Figure 1), L-malate dehydrogenase (L-MDH) catalyzes the conversion of L-malic acid and NAD^+ to oxaloacetate plus NADH. In turn, NADH transfers its hydrogen atom to the phenazine methosulphate (PMS) and 3-(4.5-dimethylthiazol-2-yl)-2.5-diphenyl tetrazolium bromide (MTT) system, reducing MTT and producing a water-insoluble purple-colored MTT formazan. In turn, aspartate aminotransferase (AST) catalyzes the conversion of oxaloacetate plus L-glutamate to L-aspartate and 2-oxoglutarate. Since dehydrogenation of L-malic acid into oxaloacetate catalyzed by L-MDH is a highly endergonic reaction ($\Delta G°$=+29.7 kJ/mol) [14], the addition of AST favors the consumption of oxaloacetate, which pulls the MDH reaction towards the formation of oxaloacetate.

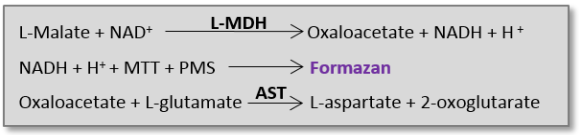

Figure 1. Reaction scheme of the colorimetric system developed to detect L-malic acid. NADH produce reacts with the PMS-MTT resulting in a purple product in the presence of the analyte.

3.2 Analytical Performance

The ability of a µPAD to detect different amounts of L-malic acid was tested. Standards with various concentrations of substrate were added to each spot and allowed to dry on air. Spots were then digitalized and analyzed. The color developed within each spot with the increasing concentration of substrate is shown on the top of Figure 2A. While in the absence of L-malic acid no signal is obtained, with the increase in the concentration of L-malic acid a color change occurs, increasing the purple tint. Thus, it is possible to perform a semi-quantitative analyzes by visual read-out. However this is only reliable for concentrations higher than 20 mg/L of L-malic acid, where the differences between concentrations are evident. A plot with the mean grey intensity determined as a function of L-malic acid concentration is shown in Figure 2A. The average mean grey intensity increases with the increasing concentration of substrate reaching a saturation point at 200 mg/L of L-malic acid. Assay linearity was also assessed by plotting the average grey mean intensity as a function of the logarithm of the concentration of L-malic acid (see Figure 2B). This assay is linear from 5 to 150 mg/L with a correlation coefficient of 0.984. The relative standard deviations calculated for all concentrations were in the range of 0.9 – 3.5 mg/L (n = 5), representing a notorious precision of the method. Thus, the method was found suitable for a quantitative analyze of samples with concentrations within the range of 5 to 150 mg/L. The limit of detection (LOD) of L-malic acid obtained was 5.8 mg/L, which is higher to the value reported for the L-

malic acid, UV method protocol from NZYTech. On the other hand, the limit of quantification (LOQ) was equal to 19.8 mg/L.

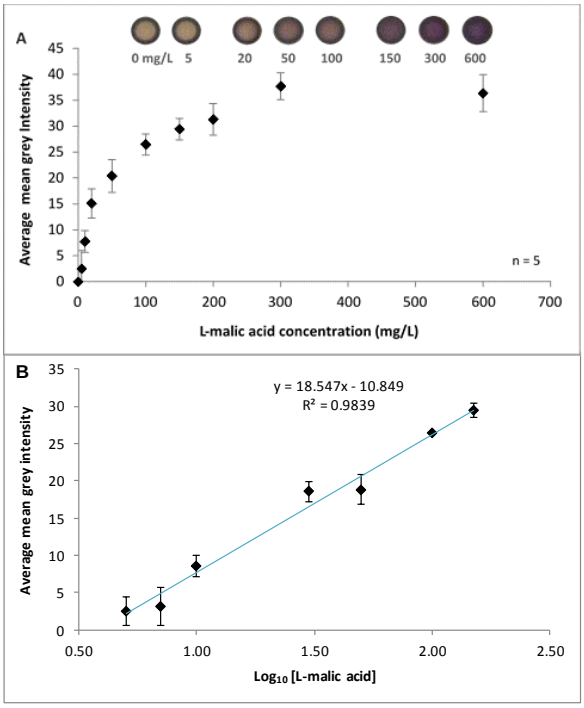

Figure 2 Analytical performance of the bioassay developed to detect L-malic acid using enzymes physically adsorbed onto a µPAD. A) Colors developed with increasing amount of L-malic acid that range from 0 to 600 mg/L. Calibration curve obtained measuring the average mean grey intensity of each spot with the corresponding concentration (n = 5). B) Assay linearity between concentrations of 5 and 150 mg/L of l-malic acid with an equation of y = 18.547 $\log_{10}$ [L-malic acid] – 10.849. Errors were always determined from the standard deviation of n = 5 measurements.

3.3 Time course stability

Bioassay stability overtime was studied, by preparing µPADs and storing them at room temperature and 4 ºC. Through time, the control started to develop a brown color regardless of the presence of the substrate, indicating a loss of stability and authenticity. Therefore, time course stability for the detection of 150 mg/L of L-malic acid was analyzed using the following equation:

$$I = \frac{I_x - I_{Cx}}{I_0 - I_{C0}} \quad \textbf{(1)}$$

where I_{C0} and I_{Cx} represent the signal intensity obtained for the control on day 1 and on day x, respectively, while I_x and I_0 represent the average mean grey intensity determined for the analyte on the day x and day 1, respectively. After 4 days of storage at RT, the device lost 88 % of activity and after 7 days was no longer viable. However, when stored at 4 ºC the device remained functional for up to 18 days, but with 26 % of the initial activity.

3.4 Adaptation to a lateral flow test

One of major features of µPADs is their simplicity and user friendliness. In order to have NAD^+ spotted onto paper, a new µPAD design was developed with 38.7 mm x 6 mm and 6-mm compartments (Figure 3). After sample addition, liquid flows via capillarity to the reaction zone, dragging NAD^+.

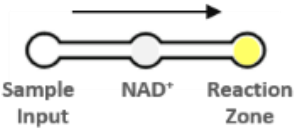

Figure 3. Schematic representation of a lateral-flow µPAD that allows the deposition of all the reagents needed for the assay. Sample is added, drags NAD^+ and reaches the reaction zone by capillary forces. The arrow represents flow direction.

This µPAD was tested by adding standard solutions of L-malic acid into the sample input. The devices were incubated in a petri dish at RT. Although a color change occurred in the presence of L-malic acid, a gradient in the color developed with the increasing concentration of L-malic acid could not be visualized. Moreover, inhomogeneity of the color distribution, which is typical on lateral-flow tests, was observed, which made it difficult to have a visual read-out and quantitative analysis. This phenomenon occurs because the pre-added enzymes are adsorbed to the porous structure of paper by electrostatic interactions. Thus, upon sample addition, enzymes and other components may desorb back into the fluid, migrating further to the edges of the reaction zone [15]. Therefore, one of the goals of this work is to immobilize both AST and MDH enzymes onto paper using CBM3 module, in order to distribute the color developed across the whole reaction zone.

3.5 Cloning, expression and purification of AST-CBM3

Fusion technology allows the combination of CBM and an enzyme of interest, in this case both MDH and AST. After several attempts to engineer pET21a_MDH-CBM3, the cloning method was not successfully achieved. In contrast, the engineered pET21a_AST-CBM3 was obtained by cloning a *cbm3* gene from pET21a_ZZ-CBM3 into pET21a_AST with a final size of 7074 bp (Figure 4A lane 2). To confirm the cloning, a digestion with XhoI enzyme was performed, followed by an agarose gel electrophoresis. In Figure 4A lane 3, it is possible to notice the presence of two fragments, one with 6561 bp and another with 513 pb fragment, which corresponds to pET21a_AST and to *cbm3* gene, respectively. The construction was also confirmed by sequencing.

Expression and purification of AST-CBM3 were confirmed by SDS-PAGE. AST was also expressed and purified as a control. Lanes 6 and 9 in the SDS-PAGE gel of Figure 4B correspond to AST and AST-CBM3 purified fractions, respectively. The molecular weight of the AST and CBM3 partners of the fusion protein are 45 kDa and 17.6 kDa, respectively. The fusion protein is well expressed in *E. coli* BL21(DE3) strains with the expected protein weight of approximately 63.5 kDa (predicted using ExPASYs Compute pI/Mw). Purified AST protein and AST-CBM3 have a final concentration of 9 µM and 42 µM, respectively.

3.6 Binding of AST-CBM3 to cellulose

CBM3 from *C. thermocellum* is known for its high affinity to cellulose, so the capability of AST-CBM3 to bind Whatman No. 1 filter paper was evaluated and compared with AST and CBM3. The amount of moles of enzyme adsorbed per gram of paper is shown in Figure 5. AST-CBM3 ability to bind cellulose is

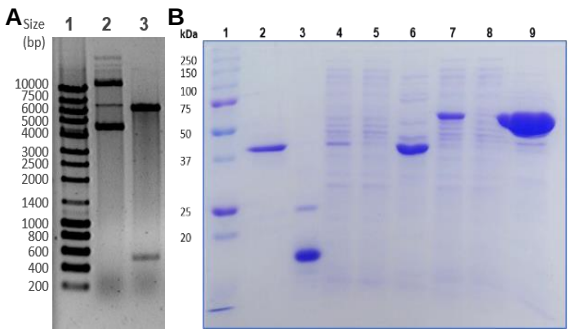

Figure 4. A) Agarose gel analysis of pET21a_AST-CBM3 cloning. 1. NZYDNA Ladder III; 2. pET21a_AST-CBM3; 3. pET21a_AST-CBM3 previously digested with XhoI. B) Coomassie Blue stained SDS-PAGE of fractions collected during purification of AST and AST-CBM3. 1. Precision Plus Protein™ Dual Color Standard; 2. AST from NZYTech; 3. CBM3; 4. Feed sample for AST purification; 5. Flow-through fraction of AST purification; 6. Elution fraction of AST protein; 7. Feed sample for AST-CBM3 protein purification; 8. Flow-through fraction of AST-CBM3 purification; 9. Elution fraction of AST-CBM3 protein.

approximately 2-folds higher than AST protein without CBM3, but 1.4-folds lower when compared with CBM3. Binding of AST-CBM3 was inferior to CBM3, most likely due to the tertiary structure adopted by the fusion-protein. Cellulose-binding amino-acid residues of the planar strip of CBM3 may not all be on the surface of the protein and available to establish interactions with cellulose. Still, these results show that the CBM3 domain of the fusion protein is active and with a high cellulose binding capacity.

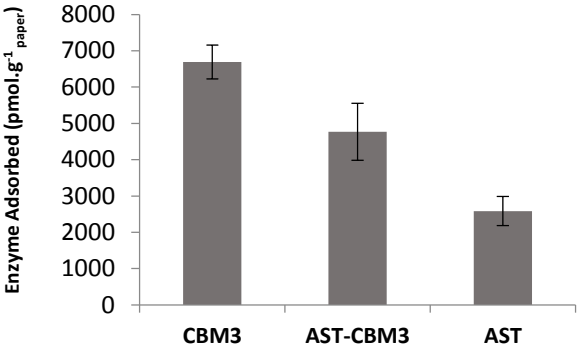

Figure 5. Binding capacity of AST-CBM3, AST and CBM3 proteins to cellulose at pH 10. Each protein was added to a filter plate with 2 paper spots with 0.009 g each. Errors were determined from the standard deviation of triplicates.

3.7 Activity of AST-CBM3 on paper

AST-CBM3 catalytic activity was assessed and compared with AST using µPADs with 6 mm spots

and the colorimetric assay developed. It was noticed that both the reactions with AST-CBM3 and AST in imidazole buffer are faster than AST in ammonium sulfate (provided by NZYTech) resulting in a more intense purple color.

The analytical performance of the µPAD with AST-CBM3 was evaluated. In Figure 6A, it is evident that more intense colors develops with increasing concentration of substrate when compared with Figure 2A. A plot with the mean grey intensity determined as a function of L-malic acid concentration deposited is each spot is shown in Figure 6A. The increase of the average mean grey intensity with the increasing concentration of substrate reached the same saturation point (at 200 mg/L) that when using AST. However, in this case the average grey mean intensity is a linear function of the concentration of L-malic acid (see Figure 6B). This assay is linear from 5 to 150 mg/L with a correlation coefficient of 0.987. Moreover, the relative standard deviation calculated for all concentrations was in the range of 2 – 5.5 mg/L (n = 5), which is slightly higher than when using AST (0.9 – 3.5 mg/L). Thus, the method precision was retained. In this case, LOD and LOQ values of 9.2 mg/L and 30.7 mg/L were determined, respectively. These values are slightly higher than those reported before for AST and also than those described for the L-malic acid, UV method protocol from NZYTech [16]. All the previous results show that AST-CBM3 does not affect the bioassay analytical performance, meaning that the AST domain from the fusion protein retain its intrinsic biological activity.

Sometimes, for the final user a semi-quantitative analysis is enough for most purposes. In this case, a calibration chart was designed taking into account the concentrations whose color development are sufficiently different to make an accurate interpretation of the results (Figure 7). A semi-quantitative analysis is possible from 20 mg/L of L-malic acid and by visual comparison with the colored calibration chart represented in Figure 7.

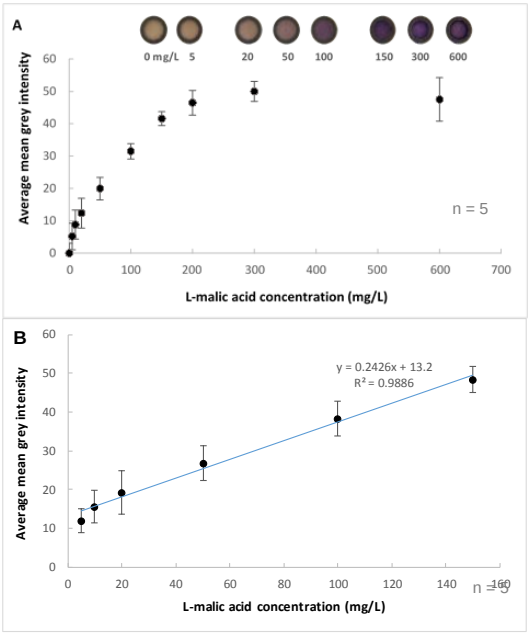

Figure 6. Analytical performance of the bioassay developed to detect L-malic acid using AST-CBM3 and MDH enzymes immobilized onto a µPAD. A) Colors developed with increasing amount of L-malic acid that range from 0 to 600 mg/L. The respective calibration curve obtained by measuring the average mean grey intensity of each spot (n = 5). B) Assay linearity between concentrations of 5 and 150 mg/L of L-malic acid with an equation of y = 0.2426 [L-malic acid] + 13.2. Errors were always determined from the standard deviation of n = 5 measurements.

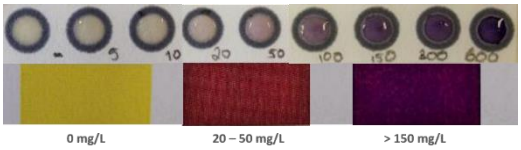

Figure 7. Calibration chart designed for L-malic acid detection assay using µPADs with AST-CBM3 fusion.

The shelf-life of µPADs prepared with AST-CBM3 and AST in imidazole were compared during storage at RT and 4 ºC. Each spot was tested with 0 and 150 mg/L of L-malic acid over a period of several days. Figure 8A shows that after 4 days of storage at RT, µPADs with AST-CBM3 or AST still have 50 % of the initial activity. The devices were active up to 14 days. Enzymes in imidazole are more stable at room temperature than AST in ammonium sulfate (data not shown). When stored at 4 ºC, no significant differences between AST and AST-CBM3 µPADs

were visible (Figure 8B). Devices were active for 18 days, conserving ~60 % of the initial activity, which contrasts with the 26 % activity of AST in ammonium sulfate (see section 3.3).

The effect of AST-CBM3 on a lateral flow µPAD was also evaluated. However, AST-CBM3 had no impact on the inhomogeneity of the color distribution typical in lateral flow tests. Still, it is believed that the use of both enzymes fused with CBM3 will overcome this limitation and redistribute the color development across the whole reaction zone.

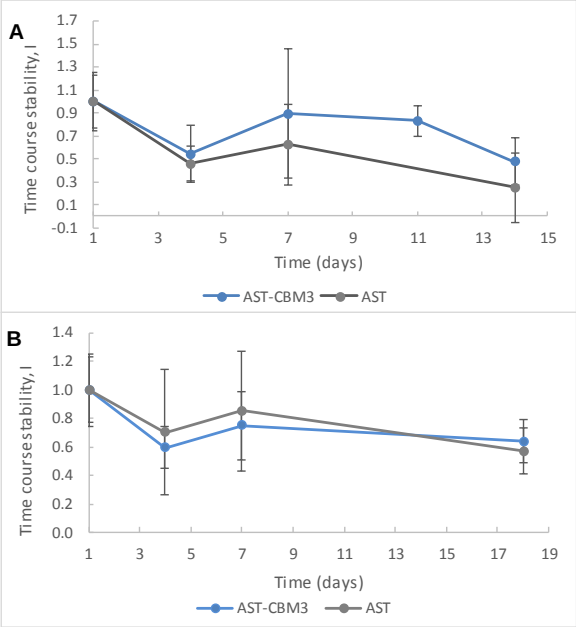

Figure 8. Time course stability of the bioassay using AST or AST-CBM3. Pre-prepared spots were incubated at 4 ºC and RT in the dark. Time course stability was determined according with equation 1. Error bars were determined from the standard deviations of 3 measurements for each condition.

3.8 L-malic acid detection in wine

An experimental proof of concept was performed using a µPAD functionalized with MDH and AST-CBM3 for L-malic acid detection in white and red wines. Since these µPADs rely on a colorimetric detection, a sample pre-treatment with activated carbon was performed to remove colored polyphenols (anthocyanins) from red wine. Then, 7 µL of a solution containing wine sample, NAD^+ and buffer were spotted onto a 6 mm-diameter µPAD and allowed to dry on air. A quantitative analysis was performed and the amount of L-malic acid was determined in each wine using the equation Average mean grey intensity = 0.2426 [L-malic acid] + 13.2. The results shown in Table 1 indicate that the white wines tested have a higher content of L-malic acid compared with red wines. In addition, in sample 5 it was not detected the analyte of interest. This proves that it is possible to determine L-malic acid in wine using this rapid test. To validate these results, the same wines were analyzed using L-malic acid, UV method (NZYTech, Lisbon, Portugal). As it can be observed in Table 1, a very good correlation was obtained between the two methods demonstrating that this µPAD is suitable for the detection and quantification of the analyte.

Table 1 Concentration of L-malic acid determined in white whites and red wines using µPAD and the NZYTech L-malic acid, UV detection kit. The standard deviation (SD) corresponds to triplicates.

	Sample	µPAD [L-malic acid] (mg/L ± SD)	UV [L-malic acid] (mg/L ± SD)
White wine	1	1352.0 ± 100.1	1658.3 ± 64.7
	2	1244.5 ± 22.7	1147.2 ± 146.5
	3	2097.3 ± 292.8	3120.0 ± 62.5
Red Wine	4	23.3 ± 10.3	13.1 ± 7.1
	5	0	0
	6	336.8 ± 4.9	218.1 ± 41.1

µPAD accuracy using AST-CMB3 enzyme was also evaluated by spiking analyte. Known amounts of L-malic acid (1.3, 2.5 and 5.0 mg) were added to 50 mL of white wine 3 (diluted 50 times) and red wine 4. Then, red wine was pre-treated with activated carbon. The concentration determined was then compared with the theoretical value expected (data not shown). Comparing the expected values with the experimental data, a slight decrease in the L-malic acid content is observed. Nevertheless, both wines show a high recovery percentage, so the µPAD shows a great accuracy, indicating that these device can be used for the quantitative determination of L-malic acid in the winemaking process.

4 Conclusion

Throughout the years, µPADs emerged has a promising platform for the development of expedite and inexpensive analytical solutions in developing and developed nations. This work represents the first steps in the development of an innovative µPAD to detect L-malic acid in wines. As a first approach, a colorimetric system was developed based on two enzymes, AST and MDH, and a non-enzymatic reaction, that results in a purple final product in the presence of L-malic acid. Both enzymes were physically adsorbed onto paper together with chromogenic reagents. The µPAD designed showed a good analytical performance associated with a simple and fast preparation, reliability and low limit of detection. Still, the devices retain just 26 % of their activity after 18 days of storage at 4 ºC. Moreover, the colorimetric system was adapted to a lateral-flow µPAD, where NAD^+ was spotted onto paper, but a color inhomogeneity was observed. Therefore to improve shelf-time and color homogeneity, attempts were made to fuse enzymes with a CBM3 from C. *thermocellum* to increase binding affinity towards cellulose. While AST-CBM3 was successfully cloned, problems with the MDH-CBM3 fusion were recurrent. By using the AST-CBM3 fusion in imidazole buffer, the colorimetric reaction was much faster (10 min) without affecting the good analytical performance of µPADs. µPADs with AST-CBM3 were suitable for an accurate detection of L-malic acid in wines. Semi-quantitative analysis can be achieved by visually comparing color developed with a calibration chart. If a quantitative analysis is required, a scanner and image analysis software can be used to convert the colored signal into an L-malic acid titer.

In order to accomplish the ultimate goal of developing a µPAD suitable for winemaking industry in a lateral-flow format, MDH-CBM3 fusion protein such be genetically engineered and the impact on µPAD analytical performance, self-life and color uniformity such be evaluated. Moreover, it would be interesting to develop a 3D-µPAD that could incorporate discs of activated carbon to remove red wine color just by gravity.

5 References

[1] J. H. Swiegers, E. J. Bartowsky, P. A. Henschke, and I. S. Pretorius, "Yeast and bacterial modulation of wine aroma and flavour," *Aust. J. Grape Wine Res.*, vol. 11, pp. 139–173, 2005.

[2] J. Su, T. Wang, Y. Wang, Y.-Y. Li, and H. Li, "The use of lactic acid-producing, malic acid-producing, or malic acid-degrading yeast strains for acidity adjustment in the wine industry.," *Appl. Microbiol. Biotechnol.*, vol. 98, no. 6, pp. 2395–413, 2014.

[3] S. Liu, "Malolactic fermentation in wine – beyond deacidification," *J. Appl. Microbiol.*, vol. 92, pp. 589–601, 2002.

[4] A. Costantini, E. Garc, and M. V. Moreno-arribas, "Biochemical Transformations Produced by Malolactic Fermentation," *Wine Chem. Biochem.*, vol. 1, pp. 27–58, 2009.

[5] S. Sua and F. Huidobro, "A review of the analytical methods to determine organic acids in grape juices and wines," *Food Res. Int.*, vol. 38, pp. 1175–1188, 2005.

[6] U. Regmi, M. Palma, and C. G. Barroso, "Direct determination of organic acids in wine and wine-derived products by Fourier transform infrared (FT-IR) spectroscopy and chemometric techniques.," *Anal. Chim. Acta*, vol. 732, pp. 137–44, 2012.

[7] Z. Kerem, B. Bravdo, O. Shoseyov, and Y. Tugendhaft, "Rapid liquid chromatography–ultraviolet determination of organic acids and phenolic compounds in red wine and must," *J. Chromatogr. A*, vol. 1052, no. 1–2, pp. 211–215, 2004.

[8] A. W. Martinez, S. T. Phillips, M. J. Butte, and G. M. Whitesides, "Patterned paper as a platform for inexpensive, low-volume, portable bioassays," *Angew. Chem. Int. Ed. Engl.*, vol. 46, no. 8, pp. 1318–1320, 2007.

[9] E. Carrilho, A. W. Martinez, and G. M. Whitesides, "Understanding Wax Printing : A Simple Micropatterning Process for Paper-Based Microfluidics," *Anal. Chem.*, vol. 81, no. 16, pp. 7091–7095, 2009.

[10] F. Kong and Y. F. Hu, "Biomolecule immobilization techniques for bioactive paper fabrication," *Anal. Bioanal. Chem.*, vol. 403, no. 1, pp. 7–13, 2012.

[11] S. Biology, O. Yaniv, E. Morag, E. A. Bayer, and R. Lamed, "Structure of a family 3a carbohydrate-binding module from the cellulosomal scaffoldin CipA of Clostridium thermocellum with flanking linkers : implications for cellulosome structure," *Struct. Biol. Cryst. Commun.*, vol. 69, pp. 733–737, 2013.

[12] P. Tomme, a Boraston, B. McLean, J. Kormos, a L. Creagh, K. Sturch, N. R. Gilkes, C. a Haynes, R. a Warren, and D. G. Kilburn, "Characterization and affinity applications of cellulose-binding domains.," *J. Chromatogr. B. Biomed. Sci. Appl.*, vol. 715, no. 1, pp. 283–96, 1998.

[13] A. M. M. Rosa, F. Louro, S. M. Martins, J. Inácio, A. M. Azevedo, and D. M. F. Prazeres, "Capture and detection of DNA hybrids on paper via the anchoring of antibodies with fusions of carbohydrate binding modules and ZZ-domains.," *Anal. Chem.*, vol. 86, no. 9, pp. 4340–7, 2014.

[14] D. L. Nelson and M.M. Cox, *Lehninger Principles of Biochemistry*, 4th Edit., New York: W.H. Freeman, pp. 612–613.

[15] P. D. T. Garcia, T. M. G. Cardoso, C. D. Garcia, E. Carrilho, and W. K. T. Coltro, "A handheld stamping process to fabricate microfluidic paper-based analytical devices with chemically modified surface for clinical assays," *RSC Adv.*, 2014.

[16] "NZYTech, Lda: L-malic acid, UV method catalogue number: AK00011 [Online] [Cited: September 22, 2013] https://www.nzytech.com/site/vmchk/Analytical-Test-Kits/L-Malic-acid-UV-method."